Received: 18 January 2019 | Revised: 1 March 2019 | Accepted: 4 April 2019

DOI: 10.1002/bit.26988

ARTICLE

WILEY BIOTECHNOLOGY BIOENGINEERING

Photosynthetic generation of heterologous terpenoids in cyanobacteria

Nico Betterle | Anastasios Melis

Department of Plant and Microbial Biology, University of California, Berkeley, California

Correspondence
Anastasios Melis, Department of Plant and Microbial Biology, University of California, Berkeley, CA 94720-3102, USA.
Email: melis@berkeley.edu

Abstract

The work aims to convert the secondary slow metabolism of the terpenoid biosynthetic pathway into a primary activity in cyanobacteria and to generate heterologous products using these photosynthetic microorganisms as cell factories. Case study is the production of the 10-carbon monoterpene β-phellandrene (PHL) in *Synechocystis* sp. PCC 6803 (*Synechocystis*). Barriers to this objective include the slow catalytic activity of the terpenoid metabolism enzymes that limit rates and yield of product synthesis and accumulation. "*Fusion constructs as protein overexpression vectors*" were applied in the overexpression of the geranyl diphosphate synthase (*GPPS*) and β-phellandrene synthase (*PHLS*) genes, causing accumulation of GPPS up to 4% and PHLS up to 10% of the total cellular protein. Such GPPS and PHLS protein overexpression compensated for their slow catalytic activity and enabled transformant *Synechocystis* to constitutively generate 24 mg of PHL per g biomass (2.4% PHL:biomass, w-w), a substantial improvement over earlier yields. The work showed that a systematic overexpression, at the protein level, of the terpenoid biosynthetic pathway genes is a promising approach to achieving high yields of prenyl product biosynthesis, on the way to exploiting the cellular terpenoid metabolism for commodity product generation.

KEYWORDS

fusion constructs, geranyl diphosphate synthase (GPPS), protein overexpression, terpene synthesis, β-phellandrene synthase (PHLS)

1 | INTRODUCTION

Isoprenoids, also referred to as terpenoids, represent the largest class of compounds produced in nature. More than 55,000 different molecules belonging to this family are known (Breitmaier, 2006). This extraordinary variability and potential for exploitation positions isoprenoids as useful commodity products for many diverse commercial applications, including synthetic chemistry feedstock, solvents, polymers, nature-based pharmaceuticals, nutraceuticals, flavor, and fragrance compounds, as well as renewable biofuels (Angermayr, Gorchs Rovira, & Hellingwerf, 2015; George, Alonso-Gutierrez, Keasling, & Lee, 2015; Ko, Lee, Choi, Choi, & Woo, 2019; Wang, Tang, & Bidigare, 2005).

All living organisms synthetize isoprenoids, which are considered to be products of the cellular secondary metabolism because of the slower rate and lower yield compared with that of the primary cellular metabolism. The 5-carbon (5-C) isomeric molecules dimethylallyl diphosphate (DMAPP) and isopentenyl-diphosphate (IPP) are the universal precursors of all isoprenoids (Agranoff, Eggerer, Henning, & Lynen, 1960; Lichtenthaler, 2010), comprising units that

Main conclusion: The work validates and enhances application of the concept "fusion constructs as protein overexpression vectors" in the effort to convert photosynthetic microorganisms as cell factories for terpene and other commodity product generation.

 © 2019 Wiley Periodicals, Inc.

have multiple of 5-carbon configurations. It is worth noting that two distinct and separate biosynthetic pathways evolved independently in nature to generate the universal DMAPP and IPP precursors (Agranoff et al., 1960; Lichtenthaler, 2007; Lichtenthaler, 2010). Most fermentative aerobic and anaerobic bacteria, anoxygenic photosynthetic bacteria, cyanobacteria, algae (micro & macro), and chloroplasts in all photosynthetic organisms operate the methylerythritol 4-phosphate (MEP) pathway, beginning with glyceraldehyde 3-phosphate and pyruvate metabolites. Archaea, yeast, fungi, insects, animals, and the eukaryotic plant cytosol generally operate the mevalonic acid (MVA) pathway, which begins with acetyl-CoA metabolites (Lichtenthaler, 2010; McGarvey & Croteau, 1995; Schwender, Gemünden, & Lichtenthaler, 2001).

Among isoprenoids, monoterpenes have a high commercial value for their utility in the flavor and fragrance industries, but also for their potential as renewable bio-gasoline molecules (Melis, 2017). Monoterpenes are 10-C hydrocarbon molecules and the case study of this work is the monocyclic monoterpene β-phellandrene (PHL), which is a component of plant essential oils. PHL is produced by many plants (lavender, tomato, pine, eucalyptus, grand fir, among other), where it normally accumulates to low-levels in leaf and stem trichomes. The enzyme β-phellandrene synthase (PHLS) catalyzes the conversion of the intermediate terpenoid metabolite geranyl diphosphate (GPP) into β-phellandrene (Demissie, Sarker, & Mahmoud, 2011). In turn, geranyl diphosphate is generated by the covalent head-to-tail linkage of DMAPP and IPP, a reaction catalyzed by the enzyme GPP synthase (GPPS; Lichtenthaler, 2010; Schwender et al., 2001).

Production and extraction of PHL from plants are subject to limitations, including a low yield per plant, high extraction costs, and fluctuations in feedstock supply. Extensive work was done in this lab to institute a heterologous high-capacity PHL production process via the photosynthesis of the unicellular cyanobacteria *Synechocystis* sp. PCC 6803 (*Synechocystis*). This microorganism was chosen because of the ease of genetic manipulation, the fast rate of growth and productivity, relative to essential oil-producing plants, and the ability of scaling-up the production process to enable commercial exploitation. In spite of these advantages, barriers for the high-yield production of PHL via the *Synechocystis* photosynthesis include the slow catalytic activity of the PHLS enzyme (k_{cat} ~3 s^{-1}; Demissie et al., 2011; Wise & Croteau, 1999; Zurbriggen, Kirst, & Melis, 2012) and the limited photosynthetic carbon-partitioning to the terpenoid biosynthetic pathway (~5% of the total photosynthetic carbon; Lindberg, Park, & Melis, 2010; Melis, 2013).

In the present work, efforts were made to overcome the two limitations mentioned above. The approach entailed overexpression of the GPPS and PHLS enzymes of the β-phellandrene biosynthetic pathway as a means by which to compensate for their slow catalytic activity. Heterologous installation of the MVA pathway in the cyanobacterial cell, to operate in parallel with the endogenous methylerythritol-phosphate (MEP) pathway, was also implemented as a means of enhancing the flux of endogenous substrate through the two pathways toward DMAPP and IPP pool size increase.

2 | MATERIALS AND METHODS

2.1 | *Synechocystis* strains, recombinant constructs, and culture conditions

The cyanobacterium *Synechocystis* was used as the experimental strain in this work and referred to as the wild type (WT). Production of the plant monoterpene β-phellandrene (PHL) by *Synechocystis* transformants was enabled via the heterologous expression of the codon-optimized *PHLS* gene from *Lavandula angustifolia* (lavender) (Demissie et al., 2011). Codon use optimization for expression in *Synechocystis* of the lavender *PHLS* and other genes was done using open software (https://www.idtdna.com/CodonOpt). PHLS was expressed as a fusion construct with the CpcB β-subunit of phycocyanin, which was placed in the leader sequence position (CpcB*PHLS; Formighieri & Melis, 2015). PHL synthesis was further enhanced by co-expression of the CpcB*PHLS fusion along with the MVA pathway heterologous enzymes (Formighieri & Melis, 2016). Mutant strains simultaneously overexpressing the CpcB*PHLS and the MVA heterologous pathway (Formighieri & Melis, 2016) were used as the recipient strain for the heterologous addition of the *GPPS* gene. Genes coding for kanamycin resistance (*nptI*), *GPPS2* from grand fir, and acetyl-CoA acetyl transferase (*atoB*) from *Escherichia coli* were synthesized with the nucleotide sequence as reported in the recent literature (Formighieri & Melis, 2016; Kirst, Formighieri, & Melis, 2014). The gene nucleotide sequence coding for erythromycin resistance was kindly provided by Professor Neil Hunter (Hollingshead et al., 2012).

Synechocystis transformations were made according to an established protocol (Eaton-Rye, 2011; Williams, 1988). Wild type and transformants were maintained on BG11 media supplemented with 1% agar, 10 mM TES-NaOH (pH 8.2) and 0.3% sodium thiosulfate. Liquid cultures of BG11 were buffered with both 25 mM sodium bicarbonate, pH 8.2, and 25 mM dipotassium hydrogen phosphate, pH 9, and incubated under continuous bubbling with air at 26°C. Transgenic DNA copy homoplasmy in the cells was achieved upon transformant incubation on agar in the presence of antibiotic selectable markers (30 μg/ml chloramphenicol (*cmR*), 50 μg/ml erythromycin, 25 μg/ml kanamycin, and 25 μg/ml spectinomycin). The growth of the cells was promoted by using a balanced combination of white LED bulbs supplemented with incandescent light to yield a final visible light intensity of ~100 μmol photons m^{-2} s^{-1}.

2.2 | Genomic DNA PCR analysis of *Synechocystis* transformants

Genomic DNA templates were prepared, as described (Formighieri & Melis, 2014a). A 20 μl culture aliquot was provided with an equal volume of 100% ethanol followed by brief vortexing. A 200 μl aliquot

10970290, 2019, 8, Downloaded from https://analyticalsciencejournals.onlinelibrary.wiley.com/doi/10.1002/bit.26988 by University Degli Studi Di Vero, Wiley Online Library on [25/10/2024]. See the Terms and Conditions (https://onlinelibrary.wiley.com/terms-and-conditions) on Wiley Online Library for rules of use; OA articles are governed by the applicable Creative Commons License

RIGHTSLINK

of a 10% (w/v) Chelex 100 Resin (Bio-Rad, Hercules, CA) suspension in water was added to the sample before mixing and heating at 98°C for 10 min to lyse the cells. After centrifugation at 16,000*g* for 10 min to pellet cell debris, 5 μl of the supernatant was used as a genomic DNA template in a 25 μl PCR mix. Q5 DNA polymerase (New England Biolabs, Ipswich, MA) was used to perform the genomic DNA PCR analyses. Transgenic DNA copy homoplasmy in *Synechocystis* was tested using suitable primers listed in the Supporting Information Materials. The genomic DNA location of these primers is indicated in the figures with the appropriate DNA constructs.

2.3 | Protein analysis

The cells in the mid-exponential growth phase (OD_{730} ~1) were harvested by centrifugation at 4,000*g* for 10 min. The pellet was resuspended in a solution buffered with 25 mM Tris-HCl, pH 8.2, also containing a cOmplete mini protease inhibitor cocktail (Roche, Basel, Switzerland; one 50 mg tablet was added per 50 ml suspension). The cells were broken by passing the suspension through a French press cell at 1,500 psi. A slow speed centrifugation (350*g* for 3 min) was applied to remove unbroken cells. For the protein electrophoretic analysis, samples extracts were solubilized upon incubation for 1 hr at room temperature in the presence of 125 mM Tris-HCl, pH 6.8, 3.5% SDS, 10% glycerol, 2 M urea, and 5% β-mercaptoethanol. Sodium dodecyl sulfate-polyacrylamide gel electrophoresis (SDS-PAGE) was performed using Mini-PROTEAN TGX precast gels (Bio-Rad). Densitometric quantitation of target proteins was performed using the Bio-Rad Image Lab software. SDS-resolved proteins were then transferred to a nitrocellulose membrane and Western-Blot analyses were performed by probing with rabbit-raised GPPS2, HmgR, and Pmk-specific polyclonal antibodies, as previously described (Bentley, Zurbriggen, & Melis, 2014; Formighieri & Melis, 2016).

2.4 | Quantification of β-phellandrene synthesis by *Synechocystis* transformants

Production, removal, and quantification of β-phellandrene from the cultures of *Synechocystis* transformants were performed according to previous methods established in this lab (Bentley & Melis, 2012; Formighieri & Melis, 2015). OD_{730} values of cultures were measured and, after centrifugation at 4,000*g* for 10 min, cell pellets were resuspended in fresh BG11 media to reach an OD_{730} of about 0.5 in a total volume of 500 ml. Refreshed cultures were incubated in the gaseous/aqueous two-phase bioreactor (Bentley & Melis, 2012). Aliquots of 50 ml volume were harvested from each culture to determine the biomass content (g/L) at time zero, using a gravimetric approach. Cultures were slowly bubbled for 10 s with 100% CO_2, which was sufficient to displace head-space gases and to fill the gaseous phase inside the bioreactor with CO_2. The reactors were then sealed and incubated under continuous illumination and upon gentle stirring of the culture. After 48 hr of such incubation, an aliquot of 50 ml was again harvested to determine the final dry cell weight of the biomass content. 15 ml of heptane were then added to the surface of the culture to help collect the floating terpene hydrocarbon products. The concentration of monoterpenes in the heptane extracts was quantified by UV-absorbance spectrophotometry and sensitive flame ionization detector gas chromatography (GC-FID), as previously described (Betterle & Melis, 2018; Formighieri & Melis, 2014a; Formighieri and Melis, 2014b). β-Phellandrene has a known absorbance spectrum with a primary peak at 232.4 nm in heptane. The concentration of this monoterpene was calculated applying Lambert-Beer's law (ε [232.4 nm] = 15.7 mM^{-1} cm^{-1}; Formighieri & Melis, 2014b). Total absorbance in the UV region for the various samples was then normalized to the amount of biomass (OD/w) generated during the 48-hr incubation in the bioreactor, as previously described (Betterle & Melis, 2018; Formighieri & Melis, 2016).

3 | RESULTS

3.1 | DNA constructs and operon configurations

Transformant cyanobacteria used in this work harbored three constructs, as shown in Figure 1. The phycocyanin-encoding *cpc* locus contained a fusion of the *PHLS* gene from *Lavandula angustifolia* (lavender) with the *cpcB* gene as the leader sequence, followed by the *cmR* resistance selection cassette (Figure 1, upper). Selection in the presence of chloramphenicol was applied to attain homoplasmy of transformants with the *cpcB*PHLS* fusion (please see below). Recent work from this lab (Formighieri & Melis, 2015; Formighieri & Melis, 2016; Kirst et al., 2014) showed that such transformants cannot assemble phycocyanin and possess a truncated phycobilisome antenna size comprising the allophycocyanin core only (not shown here).

The *psbA2* locus contained an operon of the upper MVA 3-hydroxy-3-methylglutaryl-CoA synthase (*hmgS*), 3-hydroxy-3-methylglutaryl-CoA reductase (*hmgR*), and acetyl-CoA transferase (*atoB*) genes, plus the erythromycin (*ermC*) selectable marker, operated under the control of the native P_{psbA2} promoter (Figure 1, middle). Selection in the presence of erythromycin was applied to attain homoplasmy of transformants with the upper MVA operon (please see below). The *psbA2* gene, encoding the D1–2 variant of the 32 kD photosystem II reaction center protein, was replaced by this operon in these transformants.

The *glgA1* locus contained a fusion of the *GPPS* gene from *Picea abies* (Norway spruce) with the kanamycin (*nptI*) resistance gene as the leader sequence (Figure 1, lower). The *nptI*GPPS* fusion was shown to confer kanamycin resistance while amplifying protein expression of this construct (Betterle & Melis, 2018). The *nptI*GPPS* fusion construct was followed in an operon configuration by genes of the lower the MVA pathway, including isopentenyl-diphosphate isomerase (*fni*), mevalonic acid kinase (*mk*), di-phospho-mevalonic acid decarboxylase (*pmd*), and phospho-mevalonic acid kinase (*pmk*), plus the spectinomycin (*smR*) selectable marker. This operon was

RIGHTSLINK

10970290, 2019, 8, Downloaded from https://analyticalsciencejournals.onlinelibrary.wiley.com/doi/10.1002/bit.26988 by University Degli Studi Di Vero, Wiley Online Library on [25/10/2024]. See the Terms and Conditions (https://onlinelibrary.wiley.com/terms-and-conditions) on Wiley Online Library for rules of use; OA articles are governed by the applicable Creative Commons License

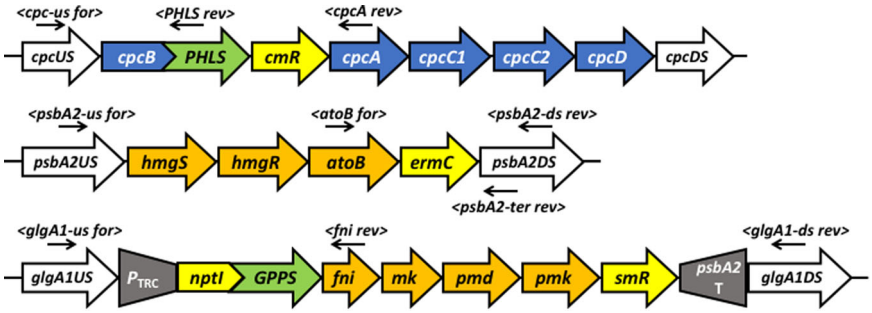

FIGURE 1 Schematic presentation of the recombinant operon constructs expressed in *Synechocystis*. (Upper) Insertion of the lavender *PHLS* gene in a fusion construct configuration with the phycocyanin β-subunit *cpcB* gene as the leader sequence. The *cpcB*PHLS* fusion construct was inserted in the *cpc* operon and expressed under control of the *cpc* promoter and chloramphenicol resistance cassette *cmR*. (Middle) Upper Mevalonic acid (MVA) pathway genes replacing the endogenous *psbA2* gene, as previously described (Formighieri & Melis, 2016). The 3-hydroxy-3-methylglutaryl-CoA synthase (*hmgS*) and 3-hydroxy-3-methylglutaryl-CoA reductase (*hmgR*) gene sequences were from *Enterococcus faecalis*, whereas the acetyl-CoA acetyl transferase (*atoB*) gene was from *Escherichia coli*. Transgenes in this operon were expressed under control of the P_{psbA2} promoter and erythromycin *ermC* resistance cassette. (Lower) Lower MVA pathway genes replacing the endogenous *glgA1* gene, as previously described (Formighieri & Melis, 2016). The geranyl diphosphate synthase (*GPPS*) was from *Picea abies*. The isopentenyl-diphosphate isomerase (*fni*), mevalonic acid kinase (*mk*), di-phospho-mevalonic acid decarboxylase (*pmd*), and phospho-mevalonic acid kinase (*pmk*) genes were from *Streptococcus pneumoniae*. The *Picea abies GPPS* gene, in a fusion construct configuration with the *nptI* kanamycin resistance gene as the leader sequence (*nptI*GPPS*), was inserted as the first construct in the lower MVA operon, was expressed under control of the P_{TRC} promoter and the kanamycin resistance cassette *nptI*. Arrows mark the position of oligonucleotide primers used for genomic DNA PCR analysis. PHLS: β-phellandrene synthase [Color figure can be viewed at wileyonlinelibrary.com]

under the control of the P_{TRC} promoter (Figure 1, lower). Selection in the presence of kanamycin or spectinomycin was applied to attain homoplasmy of transformants with the lower MVA pathway (please see below). The *glgA1* gene, encoding a variant of the cyanobacterial glycogen synthase, was replaced by this operon in these transformants. Nucleotide sequences of the constructs used for the above-discussed transformations of *Synechocystis* are available in the Supporting Information Materials.

The yield of β-phellandrene in these transformant cyanobacteria, henceforth referred to as the "NptI*GPPS" strains and harboring the three constructs shown in Figure 1, was compared with that of strains harboring the *GPPS* gene in the same location of the *glgA1* operon (Figure 1) but without the *nptI* fusion configuration (Figure S1; Formighieri & Melis, 2016). The latter is simply termed as the "GPPS" strain. The objective of this work was to compare levels of protein expression of the *GPPS* gene in the "GPPS" and "NptI*GPPS" strains, and also to compare the yield of β-phellandrene production as a function of the GPPS protein expression variable.

3.2 | Homoplasmy analysis

Attainment of DNA copy homoplasmy in the NptI*GPPS transformant strains was tested by the genomic DNA PCR analysis. Primers < *cpc-us for* > and < *cpcA rev* > (Figure 1 and Table S1) generated a 1,289 bp product in the wild type and a 3,735 bp product in the transformant (Figure 2, left panel, WT, and NptI*GPPS). These results reflected amplification of the *cpcB* gene in the wild type and amplification of the larger *cpcB*PHLS* plus *cmR* genes in the mutant. Absent from the latter were wild type size products, showing attainment of DNA copy homoplasmy with respect to the *cpcB*PHLS* plus *cmR* transformant.

Primers < *psbA2-us for* > and < *psbA2-ter rev* > (Figure 1 and Table S1) generated a 1,528 bp product in the wild type and a 6,108 bp product in the transformant (Figure 2, middle panel, WT and NptI*GPPS). These results are consistent with amplification of the

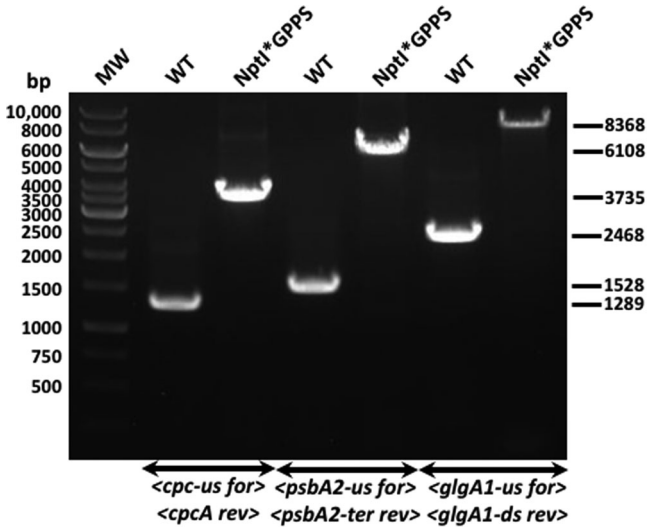

FIGURE 2 Genomic DNA PCR analysis testing for transgenic DNA copy homoplasmy in *Synechocystis* transformants. Wild type and transformant strains coexpressing the *cpcB*PHLS* fusion, the upper MVA, and the *nptI*GPPS* fusion plus lower MVA genes were probed in genomic PCR reactions for product generation and transgenic DNA segregation. Primers < *cpc-us forward* > and < *cpcA reverse* > , < *psbA2-us forward* > and < *psbA2 ter reverse* > , and < *glgA1-us forward* > and < *glgA1-ds reverse* > showed substantially different and unique products in the wild type and the transformants comprising the three operons of Figure 1, offering evidence of DNA copy homoplasmy for the transformants. GPPS: geranyl diphosphate synthase; MVA: mevalonic acid; WT: wild type

10970290, 2019, 8, Downloaded from https://analyticalsciencejournals.onlinelibrary.wiley.com/doi/10.1002/bit.26988 by University Degli Studi Di Vero, Wiley Online Library on [25/10/2024]. See the Terms and Conditions (https://onlinelibrary.wiley.com/terms-and-conditions) on Wiley Online Library for rules of use; OA articles are governed by the applicable Creative Commons License

RIGHTSLINK

psbA2 gene in the wild type and amplification of the much larger upper MVA operon plus *ermC* genes in the transformant. Absent from the latter were wild type size products, showing attainment of DNA copy homoplasmy with respect to the upper MVA operon in the transformant.

Primers < *glgA1-us for* > and < *glgA1-ds rev* > (Figure 1 and Table S1) generated a 2,468 bp product in the wild type and an 8,368 bp product in the transformant (Figure 2, right panel, WT and NptI*GPPS). These results are consistent with amplification of the *glgA1* gene in the wild type and amplification of the much larger *nptI*GPPS*, lower MVA operon, plus *smR* genes in the transformants. Absent from the latter were wild type size products, showing attainment of DNA copy homoplasmy with respect to the *nptI*GPPS*, lower MVA operon, plus *smR* transformant.

Also important in the context of this work was the necessity to probe for the presence of the specific transgenes (Figure 1) with primers drawn from within the DNA sequences of these transgenes. This was tested in genomic DNA PCR reactions of the transformant strain, first with primers < *cpc us for* > and < *PHLS rev* > (Figure 1 and Table S1), which are respectively annealing the region between the *cpc* operon upstream region and the exogenous *PHLS* gene in the *cpcB*PHLS* fusion construct. This PCR approach amplified a 1,927 bp product (Figure 3, PHLS), showing the expected product size and affirming the presence of the heterologous *PHLS* gene. Primers < *atoB for* > and < *psbA2-ds rev* > (Figure 1 and Table S1) amplified an 1,897 bp product (Figure 3, U-MVA), showing the expected product size and presence of a component of the upper MVA pathway (the *atoB* gene) in this locus. Primers < *glgA1-us for* > and < *fni rev* > (Figure 1 and Table S1) amplified a 2,515 bp product (Figure 3, L-MVA), showing the expected product size and affirming the presence of a component of the lower MVA pathway (the *fni* gene) in this locus.

The systematic genomic DNA PCR analysis conducted (Figures 2 and 3) provided evidence of DNA copy homoplasmy for the three constructs shown in Figure 1 and also provided evidence for the presence of at least one transgene in each of the respective operons, thereby strengthening the notion of the proper integration of the three operons in the genomic DNA of the transformant *Synechocystis* strains.

3.3 | Strain protein analysis

The main target of this work was to obtain a transformant that combined presence of the MVA pathway enzymes together with highly-expressed PHLS and GPPS enzymes. In this quest, a cellular protein content analysis was conducted to compare the PHLS and GPPS protein expression levels in three independent *Synechocystis* lines, harboring the three operons shown in Figure 1 and containing either the *GPPS* gene in the lower MVA pathway operon, as presented by Formighieri and Melis (2016) (Figure S1), or the *nptI*GPPS* fusion construct, as shown in Figure 1. The SDS-PAGE Coomassie stain of *Synechocystis* total protein extracts is shown in Figure 4(a). The untransformed wild type (WT) showed abundant protein bands migrating to ~19 and 14 kD, representing the CpcB β-subunit and CpcA α-subunit of phycocyanin, respectively (Figure 4a, WT).

Three independent *Synechocystis* lines, harboring the three operons with the GPPS gene in the lower MVA pathway operon (Figure S1, (Formighieri & Melis, 2016)) showed an SDS-PAGE protein profile dominated by a band at ~75 kD, attributed to overexpression of the heterologous CpcB*PHLS fusion protein (Formighieri & Melis, 2015), as well as ~56 kD RbcL attributed to the large subunit of the Rubisco, and ~23 kD CmR attributed to the expression of the chloramphenicol resistance protein (Figure 4a, GPPS 1–3). It is important to note the lack of the CpcB and CpcA phycocyanin subunits in all of these transformants, as the phycobilisome is not assembled in strains expressing the CpcB*PHLS fusion protein (Formighieri & Melis, 2015). Expression of the GPPS transgene at ~30 kD could not be observed in the SDS-PAGE analysis of the GPPS (1–3) transformant lines (Formighieri & Melis, 2016).

Three independent *Synechocystis* lines, harboring the *nptI*GPPS* fusion construct in the lower MVA pathway operon, as presented in

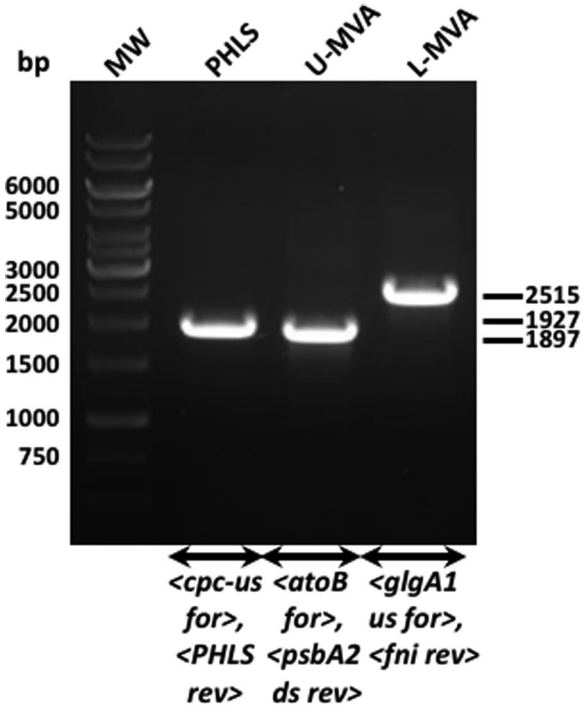

FIGURE 3 Genomic DNA PCR analysis testing for the presence of specific transgenes in *Synechocystis* transformants. Transformant strains endowed with the three operons (Figure 1) were tested for the presence of selected genes in these operons by the genomic DNA PCR analysis. Primers < *cpc-us forward* > and < *PHLS reverse* > generated the expected 1,927 bp product, showing the presence of the *PHLS* transgene in the *cpc* locus. Primers < *atoB forward* > and < *psbA2 reverse* > generated the expected 1,897 bp product, showing the presence of the *atoB* transgene in the upper MVA operon. Primers < *glgA1-us forward* and *fni reverse* > generated the expected 2,515 bp product, showing the presence of the *fni* transgene in the lower MVA operon. MVA: mevalonic acid; PHLS: β-phellandrene synthase

RIGHTSLINK

10970290, 2019, 8, Downloaded from https://analyticalsciencejournals.onlinelibrary.wiley.com/doi/10.1002/bit.26988 by University Degli Studi Di Vero, Wiley Online Library on [25/10/2024]. See the Terms and Conditions (https://onlinelibrary.wiley.com/terms-and-conditions) on Wiley Online Library for rules of use; OA articles are governed by the applicable Creative Commons License

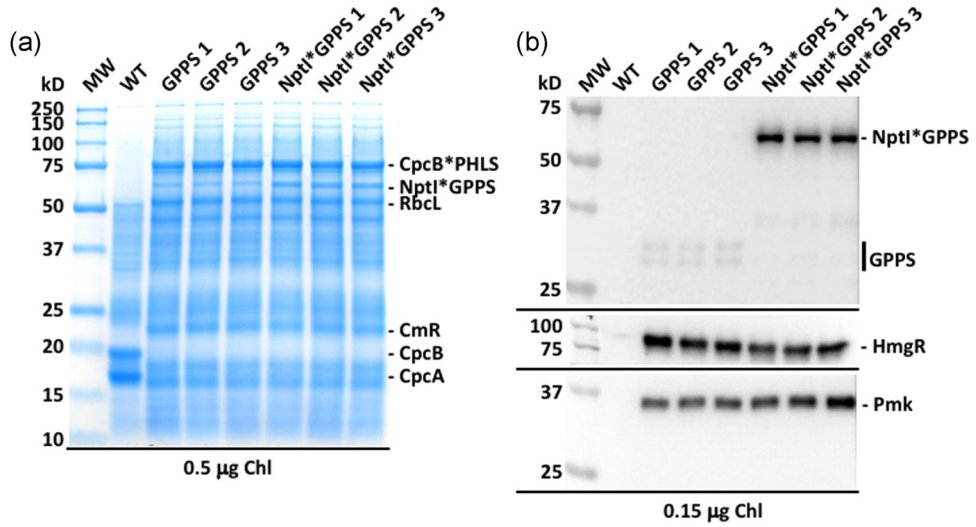

FIGURE 4 Protein expression analysis of *Synechocystis* wild type and transformants. (a) Total cellular protein extracts were resolved by SDS-PAGE and visualized by Coomassie stain. Extract of wild type *Synechocystis* cells was referred to as WT. Transformant strains referred to as GPPS denote the presence of the *GPPS* gene in the lower MVA operon (Figure S1). Transformant strains referred to as NptI*GPPS denote the presence of the fusion *NptI*GPPS* transgene in the lower MVA operon (Figure 1). Extracts from three independent lines harboring the GPPS and fusion NptI*GPPS in the lower MVA operon were loaded in the lanes of the SDS-PAGE. Individual native and heterologous proteins of interest are indicated to the right of the gel. Sample loading corresponds to 0.5 µg of chlorophyll. (b) Total protein extracts were separated by SDS-PAGE and transferred to nitrocellulose membrane for Western-blot analysis. SDS-PAGE-loaded samples were the same as in Figure 4a. Antibodies against the GPPS2 (upper panel), HmgR (middle panel) and Pmk (lower panel) were used to probe target proteins. Sample loading corresponds to 0.15 µg of chlorophyll. GPPS: geranyl diphosphate synthase; SDS-PAGE: sodium dodecyl sulfate-polyacrylamide gel electrophoresis [Color figure can be viewed at wileyonlinelibrary.com]

Figure 1, showed an SDS-PAGE protein profile also dominated by a band at ~75 kD, attributed to overexpression of the heterologous CpcB*PHLS fusion protein (Formighieri & Melis, 2015), as well as ~56 kD RbcL attributed to the large subunit of the Rubisco, and ~23 kD CmR attributed to the expression of the chloramphenicol resistance protein. Coomassie stain levels of the CpcB*PHLS fusion protein accounted for about 10.7% of the total cellular protein, exceeding the 7.3% total RbcL protein in the cells. Densitometric quantitation of target proteins was performed using the Bio-Rad Image Lab software. In addition, strains harboring the *nptI*GPPS* fusion construct (Figure 4a, NptI*GPPS 1–3) showed a substantial presence of a ~62 kD protein band, attributed to overexpression of the NptI*GPPS fusion construct (Betterle & Melis, 2018). Coomassie stain levels of this ~62 kD protein accounted for about 2.5–3.5% of the total cellular protein, approaching the level of the RbcL protein in the cells. This is the first time in related literature (Bentley et al., 2014; Formighieri & Melis, 2016) that a heterologous GPPS construct has been substantially overexpressed at the protein level in transformant cyanobacteria carrying the three operons.

Western-blot analysis with specific polyclonal antibodies was conducted to positively identify the various protein bands expressed by the *Synechocystis* lines shown in Figure 4a. Specific polyclonal antibodies against the *Picea abies* GPPS2 protein (Formighieri & Melis, 2016) failed to recognize any protein in the WT. They showed a presence of faint bands in the ~30 kD region in the GPPS lines, and further showed a strong cross-reaction with a protein migrating to ~62 kD in the NptI*GPPS fusion lines (Figure 4b). The ~30 kD region cross-reaction is attributed to the low-level expression of the *GPPS* gene in these lines. The strong ~62 kD region cross-reaction is attributed to the high-level protein expression of the *nptI*GPPS* gene in the transformant lines examined in this work.

Western blot analysis with specific polyclonal antibodies against the HmgR protein, encoded by the upper MVA pathway (Figure 1, middle), and against the Pmk protein encoded by the lower MVA pathway (Figure 1, lower), showed the presence of these proteins in both the GPPS strains (Figure 4b, GPPS 1–3; (Formighieri & Melis, 2016)) as well as in the three independent transformant lines used in this work (Figure 4b, nptI*GPPS 1–3). These results showed that overexpression of the *nptI*GPPS* gene as part of the *glgA1* locus operon has not negatively affected the heterologous expression of the MVA pathway genes.

3.4 | Biomass accumulation and β-phellandrene production

Wild type and transformants were grown photo-autotrophically under continuous illumination having a photosynthetically active radiation (PAR) intensity of ~100 µmol photons m^{-2} s^{-1} (for details, please see Material and methods section). The rate of biomass accumulation was measured from the density of the cultures at 730 nm, OD_{730} (Figure 5a). Wild type cells (WT) showed a relatively faster rate of biomass accumulation, compared with the GPPS and NptI*GPPS transformants, which showed a relatively slower rate. More specifically, the OD_{730} density curves of the three different strains indicated that, under these experimental conditions, the GPPS

RIGHTSLINK

10970290, 2019, 8, Downloaded from https://analyticalsciencejournals.onlinelibrary.wiley.com/doi/10.1002/bit.26980 by University Degli Studi Di Vero, Wiley Online Library on [25/10/2024]. See the Terms and Conditions (https://onlinelibrary.wiley.com/terms-and-conditions) on Wiley Online Library for rules of use; OA articles are governed by the applicable Creative Commons License

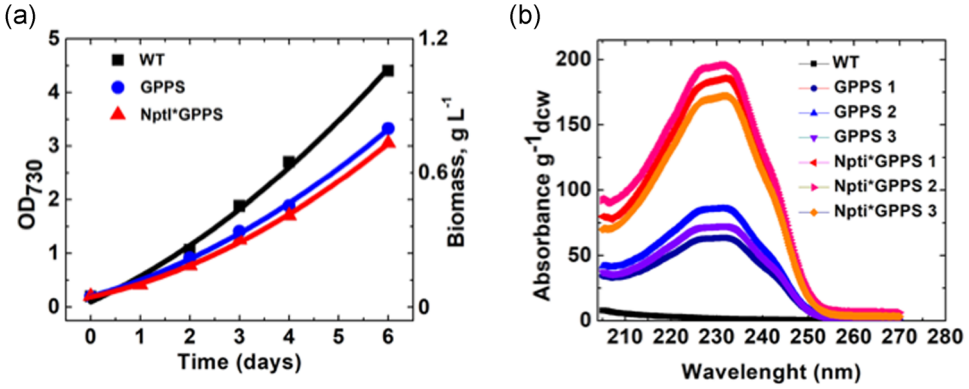

FIGURE 5 Biomass accumulation and phellandrene productivity. (a) Biomass accumulation curves of *Synechocystis* wild type and transformants, as measured from the optical density of the cultures at 730 nm (OD_{730}) and from the dry cell weight gravimetrically. Wild type *Synechocystis* (WT) and transformant lines coexpressing the CpcB*PHLS fusion protein along with the MVA pathway enzymes and the GPPS or NptI*GPPS fusion protein were analyzed. Autotrophic growth of the cells was promoted under continuous illumination (100 µmol photons m^{-2} s^{-1}). Cultures were inoculated to an initial cell concentration corresponding to OD_{730} 0.2. Such kinetic measurements were repeated yielding similar results. Average experimental errors corresponded to ± 15% (b) UV-absorbance spectra of heptane extracts from the surface of *Synechocystis* cultures. Analyzed strains were the same as in Figure 5a. The productivity of the wild type plus that of three independent lines for each transformant strain (GPPS and NptI*GPPS fusion protein) was included in these measurements. Absorbance spectra of the heptane extracts were normalized on a per g dry cell weight (dcw) of the photosynthesizing biomass generated during the culture incubation period. For more details, please see Material and methods. GPPS: geranyl diphosphate synthase [Color figure can be viewed at wileyonlinelibrary.com]

and NptI*GPPS transformants accumulated biomass with only about 70% the yield displayed by the wild type (Figure 5a). This is explained by the light irradiance used in this biomass accumulation experiment (~100 µmol photons m^{-2} s^{-1}), which is below saturation level for the rate of *Synechocystis* photosynthesis (Kirst et al., 2014). As the GPPS and NptI*GPPS transformants failed to assemble functional phycocyanin peripheral rods (Formighieri & Melis, 2015; Kirst et al., 2014), they possessed a truncated light-harvesting antenna size (TLA-phenotype). TLA-strains in low-density cultures under sub-saturating illumination are subject to slower rates of light absorption by their photosystems (Formighieri & Melis, 2015; Kirst et al., 2014), translating into slower rates of photosynthesis, productivity, growth, and biomass accumulation. In addition, the difference in growth rate between producing mutants and WT could be explained in part by the burden of deflecting endogenous carbon from cell biomass to the heterologous terpene product, as recently described for lactate producing cyanobacteria (Du et al., 2017). It is noteworthy that the substantially different composition of the antenna apparatus in wild type and NptI*GPPS transformant cells did not significantly impact the OD_{730} measurements *per se*. We compared the gravimetrical dry cell weight (dcw) accumulation as a function of OD_{730} readings of the WT and NptI*GPPS cultures (Figure S2). The slope of the linear regressions showed a strict correlation between dcw measurements and OD_{730} in both wild type (Figure S2, upper panel) and NptI*GPPS cultures (Figure S2, lower panel). The results indeed showed that the wild type accumulated biomass at 0.214 g L^{-1} OD^{-1}, whereas the NptI*GPPS cultures accumulated biomass at 0.210 g L^{-1} OD^{-1}.

The above-mentioned wild type and transformant lines were tested to evaluate the yield of β-phellandrene (PHL) production. The experiment was conducted using the gaseous/aqueous two-phase bioreactor, earlier designed in this lab (Bentley & Melis, 2012). This 1-L bioreactor comprised a lower liquid phase containing the growth media and cell inoculum, whereas the upper gaseous phase was loaded with 100% CO_2 to support photoautotrophic growth. After 48 hr incubation under illumination, floating hydrocarbons were collected upon addition of a known volume of organic solvent (heptane) to the top of the culture. Heptane extracts were assayed by UV-absorbance spectrophotometry and GC-FID analysis to evaluate the presence and amount of β-phellandrene. The PHL absorbance spectrum in the UV region shows an absorbance maximum at 232.4 nm (Bentley, García-Cerdán, Chen, & Melis, 2013; Betterle & Melis, 2018; Formighieri & Melis, 2015; Formighieri & Melis, 2016). The spectrophotometric analysis of heptane extracts from the WT culture showed an absence of compounds absorbing in this UV region of the spectrum (Figure 5b, black line). Distinct absorbance bands with a primary peak at 232.4 nm were present in the heptane extracts from both the GPPS (Figure 5b, blue lines) and NptI*GPPS transformants (Figure 5b, red lines), indicating the presence of β-phellandrene as a product of photosynthesis in these cultures. The PHL yield results were normalized to the respective cell biomass (in g dcw) that accumulated in the cultures during the 48-hr incubation under illumination. The average yield of PHL from three independent lines was calculated from the specific absorbance of β-phellandrene (for detail, please see Material and Methods section), resulting in 9.4±1.2 mg of PHL per g dcw in the GPPS cultures versus 24.0±1.6 mg of PHL per g dcw in the *nptI*GPPS* transformant cultures. These results provide evidence that a higher expression of the NptI*GPPS protein in transformants harboring the PHLS gene helped to increase the GPP pool size available to the PHLS enzyme, thus enhancing the β-phellandrene yield.

Heptane extracts were further assayed by GC-FID, To test for the identity of the hydrocarbons generated by the transformants (Figure

RIGHTSLINK
10970290, 2019, 8, Downloaded from https://analyticalsciencejournals.onlinelibrary.wiley.com/doi/10.1002/bit.26988 by University Degli Studi Di Vero, Wiley Online Library on [25/10/2024]. See the Terms and Conditions (https://onlinelibrary.wiley.com/terms-and-conditions) on Wiley Online Library for rules of use; OA articles are governed by the applicable Creative Commons License

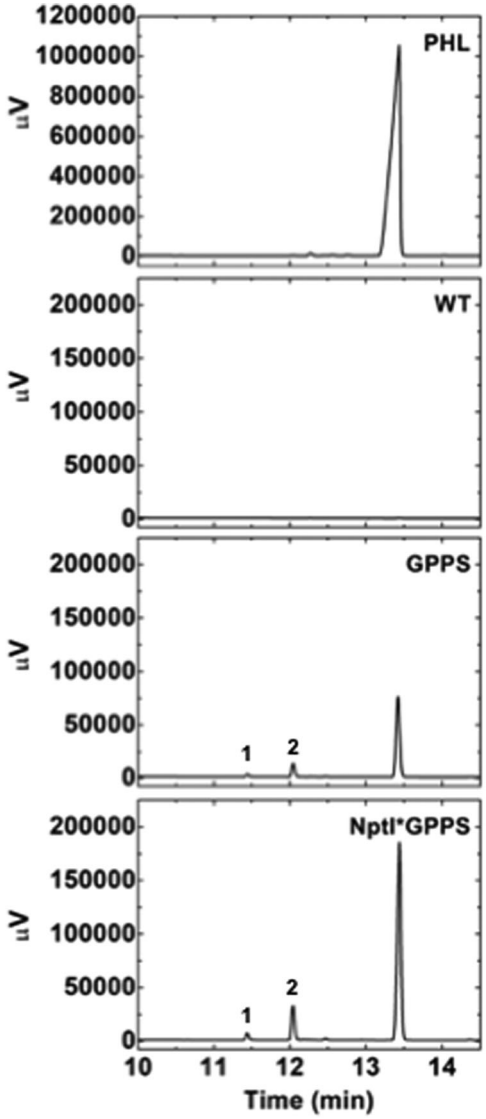

FIGURE 6 Gas chromatography (GC) with the flame ionization detector (FID) analysis of *Synechocystis* culture heptane extracts. (Upper panel) GC-FID analysis of a β-phellandrene standard (Santa Cruz Biotechnology) dissolved in heptane, showed a single peak with a retention time of 13.4 min under these experimental conditions. (Upper-middle panel) The analysis of heptane extracts from a *Synechocystis* wild type (WT) culture, showed no discernible peaks in the chromatogram. (Lower-middle panel) The analysis of heptane extracts from a *Synechocystis* transformant culture (GPPS) coexpressing the CpcB*PHLS and MVA pathway enzymes. β-Phellandrene, the major hydrocarbon product detected, showed the same retention time of 13.4 min, as the β-phellandrene standard sample. Smaller amounts of α-pinene (peak #1) and β-myrcene (peak #2) with retention times of 11.4 and 12.1 min, respectively, were also detected as nonspecific products of the CpcB*PHLS construct. (Lower panel) The analysis of heptane extracts from a *Synechocystis* transformant culture (NptI*GPPS) coexpressing the CpcB*PHLS and MVA pathway enzymes. Greater amounts of β-phellandrene (13.4 min), as well as α-pinene (11.4 min) and β-myrcene (12.1 min) were detected from the NptI*GPPS containing transformants. PHL: β-phellandrene

6). Such GC-FID analysis with a β-phellandrene standard in heptane showed a single main peak with a retention time of 13.4 min (Figure 6, PHL). Heptane extracts from the wild type did not show any peaks in the 10–14.5 min retention time range (Figure 6, WT). Heptane extract from the GPPS cultures showed a major peak at 13.4 min, attributed to PHL, as this retention time matches that of the standard (Figure 5, GPPS). Other minor peaks with shorter retention times were also present in this extract. On the basis of previous analytical work from this lab (Formighieri & Melis, 2018), these minor peaks were attributed to pinene (peak#1) and myrcene (peak#2). Qualitatively, the same chromatographic profile was observed in the heptane extract from the NptI*GPPS cultures (Figure 5, NptI*GPPS), pertaining both to the major β-phellandrene peak and the minor pinene and myrcene peaks. Of interest in this respect was the relative amplitude of the peaks attributed to β-phellandrene in the GPPS and NptI*GPPS strains. The former registered at about 86 mV units, whereas the latter was 178 mV units, that is a more than two-fold greater yield was achieved in the presence of the NptI*GPPS fusion construct.

4 | DISCUSSION

Efforts in this lab aim to transform the secondary slow metabolism of the terpenoid biosynthetic pathway into a primary activity in the cell. Achieving this objective would convert *Synechocystis*, and by extension other photosynthetic microorganisms, into cell factories for high-yield product generation. Earlier work identified two primary barriers to this objective. The first entails a regulated slow-flux of a cellular substrate through the MEP pathway toward the synthesis of terpenoids (Lindberg et al., 2010). Efforts to overcome this barrier entailed heterologous expression of the MVA pathway in *Synechocystis*, thereby coupling the primary metabolite-generating process of photosynthesis with two independent pathways (the endogenous MEP and the heterologous MVA), both working in parallel toward the synthesis of the universal terpenoid precursors DMAPP and IPP.

The second barrier entails the slow catalytic activity, which appears to be innate in enzymes of the terpenoid secondary metabolism (k_{cat} in the range of 3–4 s^{-1}). To overcome this barrier, our approach is protein overexpression, reckoning that greater abundance of the associated enzymes in the cell would compensate for their slow catalytic activity. It is noted that this was also nature's solution to the inherently slow catalytic activity of RubisCO (k_{cat} = ~3.2 s^{-1}; Sage, 2002), which is the most important enzyme of the primary photosynthetic metabolism in the cell. This necessity has made RubisCO the most abundant protein on earth (Ellis, 1979).

The general guiding principle in the field assumes that "gene overexpression" is satisfied upon the selection of a suitably strong promoter under the control of which to express the desired transgene. This may result in faster rates of transcription but not necessarily into greater amounts of the target protein (Formighieri & Melis, 2016). Unfortunately, in the vast majority of gene over-expression efforts in the literature, the corresponding level of the

10970290, 2019, 8, Downloaded from https://analyticalsciencejournals.onlinelibrary.wiley.com/doi/10.1002/bit.26988 by University Degli Studi Di Vero, Wiley Online Library on [25/10/2024]. See the Terms and Conditions (https://onlinelibrary.wiley.com/terms-and-conditions) on Wiley Online Library for rules of use; OA articles are governed by the applicable Creative Commons License

RIGHTSLINK

target protein is not quantitatively assessed at all, or only qualitatively assessed with indirect methods, such as Western blot analysis. In most cases, evidence suggests that gene expression under the control of a strong promoter does not in fact translate into substantially-greater amounts of the target protein. A novel approach in this lab applied "*fusion constructs as protein overexpression vectors*", comprising a highly-expressed gene in *Synechocystis* as a leader sequence to which the target gene was attached in C-terminus to N-terminus linear linkage. The highly-expressed leading sequence helped to enhance ribosome migration and translation through both the leading sequence and the trailing target gene in the fusion construct, resulting in an overall greater product accumulation (Chaves, Rueda-Romero, Kirst, & Melis, 2017; Formighieri & Melis, 2016). In *Synechocystis*, the highly-expressed endogenous *cpcB* gene, encoding the β-subunit of phycocyanin and also the highly-expressed heterologous *nptI* gene (Kirst et al., 2014), encoding the kanamycin resistance cassette, were used as leader sequences to overexpress the terminal *PHLS* and the preceding *GPPS* gene, respectively.

Such terpene biosynthetic gene overexpression was implemented in a *Synechocystis* strain harboring the MVA pathway in two separate operons, as recently described (Bentley et al., 2014; Formighieri & Melis, 2016). This genomic DNA configuration enabled the transformant *Synechocystis* to substantially improve levels of β-phellandrene yield by about 250% over the best achieved earlier (Formighieri & Melis, 2016). The work showed that a systematic overexpression, at the protein level, of the terpenoid biosynthetic pathway genes is a promising approach to achieving high yields of isoprenoid products. The resulting heterologous pathway installed by these genomic DNA transformations is shown in Figure 7, where CpcB*PHLS and NptI*GPPS fusion constructs, aided by the heterologous MVA pathway afford greater rates and yield of β-phellandrene production.

In more detail, past work has shown that levels of expression of the heterologous PHLS in *Synechocystis*, when in non-fusion configuration, were low regardless of the codon use optimization implemented (Bentley et al., 2013; Formighieri & Melis, 2014a). The enzyme was poorly expressed even under the control of strong native promoters (*e.g.* P_{psbA2}, P_{cpc}) to the point where the recombinant protein could not be discerned in the Coomassie-stained SDS-PAGE analysis of total cell extracts, resulting in low PHL yields. A substantial enhancement of *PHLS* expression was achieved by fusing the *PHLS* gene to the highly-expressed native *cpcB* gene, making the cpcB*PHLS fusion the most abundant protein in the cell, accounting for up to 10% of the total cellular protein (Figure 4; (Formighieri & Melis, 2015; Formighieri & Melis, 2016)). In our initial efforts, this "*fusion constructs as protein overexpression vectors*" approach and the associated greater intracellular accumulation of PHLS, enhanced the yield of PHL production from 0.025% (Formighieri & Melis, 2014a) to 0.3% (Formighieri & Melis, 2015), measured as the PHL:biomass (w:w) ratio.

However, a yield of 0.3% was still a small fraction of the photosynthetic carbon flux through the cell, given that the terpenoid biosynthetic pathway itself fluxes about 5% of all photosynthetic carbon to meet the overall prenyl needs of the cell (Lindberg et al., 2010). Similarly, low yields were reported for the production of other heterologous terpenoids in cyanobacteria (Chaves et al., 2017; Davies, Work, Beliaev, & Posewitz, 2014; Englund, Andersen-Ranberg, Miao, & Lindberg, 2015; Gao et al., 2016; Kiyota, Okuda, Ito, Yokota Hirai, & Ikeuchi, 2014; Leonard et al., 2010; Lin & Pakrasi, 2019; Lin, Saha, Zhang, & Pakrasi, 2017; Wang et al., 2016), underscoring the universal flux and yield restrictions of the process. Greater yields were recently reported for the heterologous synthesis of non-prenyl compounds, including 2,3-butanediol (Nozzi, Case, Carroll, & Atsumi, 2017), isobutanol (Miao, Xie, & Lindblad, 2018), and lactate (Du et al., 2017), underscoring the variable efficacy of different biosynthetic pathways and endogenous substrates to support carbon flux for the generation of heterologous product synthesis. To overcome the limitation of the carbon flux toward the synthesis of heterologous terpenoids; attempts to express the entire heterologous MVA pathway in *Synechocystis* were successfully conducted (Bentley et al., 2014; Formighieri & Melis, 2016). However, it was realized that expression levels and activity of the GPPS enzyme were too low to sustain a high rate of substrate flux toward the PHLS for PHL production, probably because of inability to generate a sufficient GPP pool size as the reactant of the PHLS enzyme (Formighieri & Melis, 2016). To overcome the GPPS limitation, the *fusion constructs* approach was applied in this work with the heterologous neomycin phosphotransferase (*nptI*) gene as the leader sequence to effect GPPS overexpression and, thereby, enhance the overall flux and yield of β-phellandrene production. The work showed that transformants in which both PHLS and GPPS were overexpressed the PHL:biomass carbon-partitioning ratio was more than doubled, achieving a yield of 2.4%, w-w.

Ultimately, the protein overexpression enhancement technology used in this work would have to be extended beyond the GPPS and PHLS, and applied to encompass overexpression of the MVA

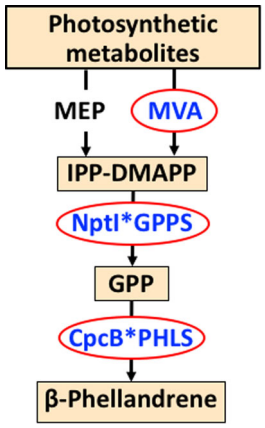

FIGURE 7 Altered terpenoid pathway flux and product generation in cyanobacteria. The endogenous methylerythritol 4-phosphate (MEP) pathway in *Synechocystis* was altered upon a genomic DNA integration of the heterologous CpcB*PHLS and NptI*GPPS fusion constructs, aided by the heterologous installation of the mevalonic acid (MVA) pathway resulting in substantial rates and yield of β-phellandrene production. PHLS: β-phellandrene synthase [Color figure can be viewed at wileyonlinelibrary.com]

RIGHTSLINK

10970290, 2019, 8, Downloaded from https://analyticalsciencejournals.onlinelibrary.wiley.com/doi/10.1002/bit.26988 by University Degli Studi Di Vero, Wiley Online Library on [25/10/2024]. See the Terms and Conditions (https://onlinelibrary.wiley.com/terms-and-conditions) on Wiley Online Library for rules of use; OA articles are governed by the applicable Creative Commons License

pathway genes from the cyanobacterial genomic DNA, and possibly that of the methylerythritol 4-phosphate pathway in the cell. Such genotypic and phenotypic alteration of photosynthetic and even non-photosynthetic organisms would create a requisite cell factory in which the secondary terpenoid metabolism has been converted to a high-yield primary biosynthetic activity in the living cell.

ACKNOWLEDGMENTS

The work was supported by University of California Berkeley Fund 45033 to Anastasios Melis.

CONFLICT OF INTERESTS

The authors declare that there are no conflicts of interest.

ORCID

Anastasios Melis http://orcid.org/0000-0003-2581-4177

REFERENCES

Agranoff, B. W., Eggerer, H., Henning, U., & Lynen, F. (1960). Biosynthesis of terpenes: VII. Isopentenyl pyrophosphate isomerase. *Journal of Biological Chemistry*, *236*, 326–332.

Angermayr, S. A., Gorchs Rovira, A., & Hellingwerf, K. J. (2015). Metabolic engineering of cyanobacteria for the synthesis of commodity products. *Trends in Biotechnology*, *33*, 352–361. https://doi.org/10.1016/j.tibtech.2015.03.009

Bentley, F. K., García-Cerdán, J. G., Chen, H.-C., & Melis, A. (2013). Paradigm of monoterpene (β-phellandrene) hydrocarbons production via photosynthesis in cyanobacteria. *Bioenergy Res*, *6*, 917–929.

Bentley, F. K., & Melis, A. (2012). Diffusion-based process for carbon dioxide uptake and isoprene emission in gaseous/aqueous two-phase photobioreactors by photosynthetic microorganisms. *Biotechnology and Bioengineering*, *109*, 100–109.

Bentley, F. K., Zurbriggen, A., & Melis, A. (2014). Heterologous expression of the mevalonic acid pathway in cyanobacteria enhances endogenous carbon partitioning to isoprene. *Molecular Plant*, *7*, 71–86. https://doi.org/10.1093/mp/sst134

Betterle, N., & Melis, A. (2018). Heterologous leader sequences in fusion constructs enhance expression of geranyl diphosphate synthase and yield of β-phellandrene production in cyanobacteria (*Synechocystis*). *ACS Synthetic Biology*, *7*, 912–921.

Breitmaier, E. (2006). *Terpenes: flavors, fragrances, pharmaca, pheromones* (223. John Wiley & Sons.

Chaves, J. E., Rueda-Romero, P., Kirst, H., & Melis, A. (2017). Engineering isoprene synthase expression and activity in cyanobacteria. *ACS Synthetic Biology*, *6*, 2281–2292.

Davies, F. K., Work, V. H., Beliaev, A. S., & Posewitz, M. C. (2014). Engineering limonene and bisabolene production in wild type and a glycogen-deficient mutant of *Synechococcus* sp. PCC 7002. *Frontiers in Bioengineering Biotechnology*, *2*, 1–11. http://journal.frontiersin.org/article/. https://doi.org/10.3389/fbioe.2014.00021/abstract

Demissie, Z. A., Sarker, L. S., & Mahmoud, S. S. (2011). Cloning and functional characterization of β-phellandrene synthase from *Lavandula angustifolia*. *Planta*, *233*, 685–696.

Du, W., Angermayr, S. A., Jongbloets, J. A., Molenaar, D., Bachmann, H., Hellingwerf, K. J., … Branco dos Santos, F. (2017). Nonhierarchical flux regulation exposes the fitness burden associated with lactate production in *Synechocystis* sp. PCC6803. *ACS Synthetic Biology*, *6*, 395–401. https://doi.org/10.1021/acssynbio.6b00235

Eaton-Rye, J. J. (2011). Construction of gene interruptions and gene deletions in the cyanobacterium *Synechocystis* sp. Strain PCC 6803. In R. Carpentier (Ed.), *Photosynthesis Research Protocols. Methods in Molecular Biology (Methods and Protocols)* 684). Totowa: Humana Press. http://link.springer.com/. https://doi.org/10.1007/978-1-60761-925-3

Ellis, R. J. (1979). The most abundant protein in the world. *Trends in Biochemical Sciences*, *4*, 241–244. http://www.cell.com/trends/biochemical-sciences/abstract/0968-0004(79)90212-3

Englund, E., Andersen-Ranberg, J., Miao, R., & Lindberg, P. (2015). Metabolic engineering of *Synechocystis* sp. PCC 6803 for production of the plant diterpenoid manoyl oxide.

Formighieri, C., & Melis, A. (2014a). Regulation of β-phellandrene synthase gene expression, recombinant protein accumulation, and monoterpene hydrocarbons production in *Synechocystis* transformants. *Planta*, *240*, 309–324.

Formighieri, C., & Melis, A. (2014b). Carbon partitioning to the terpenoid biosynthetic pathway enables heterologous β-phellandrene production in *Escherichia coli* cultures. *Archives of Microbiology*, *196*, 853–861.

Formighieri, C., & Melis, A. (2015). A phycocyanin°phellandrene synthase fusion enhances recombinant protein expression and β-phellandrene (monoterpene) hydrocarbons production in *Synechocystis* (cyanobacteria). *Metabolic Engineering*, *32*, 116–124. https://doi.org/10.1016/j.ymben.2015.09.010

Formighieri, C., & Melis, A. (2016). Sustainable heterologous production of terpene hydrocarbons in cyanobacteria. *Photosynthesis Research*, *130*, 123–135.

Formighieri, C., & Melis, A. (2018). Cyanobacterial production of plant essential oils. *Planta*, *248*, 933–946. https://doi.org/10.1007/s00425-018-2948-0

Gao, X., Gao, F., Liu, D., Zhang, H., Nie, X., & Yang, C. (2016). Engineering the methylerythritol phosphate pathway in cyanobacteria for photosynthetic isoprene production from CO_2. *Energy & Environmental Science*, *9*, 1400–1411.

George, K. W., Alonso-Gutierrez, J., Keasling, J. D., & Lee, T. S. (2015). isoprenoid drugs, biofuels, and chemicals---artemisinin, farnesene, and beyond. In J. Schrader, & J. Bohlmann (Eds.), *Biotechnol. Isoprenoids* (pp. 355–389). Cham: Springer International Publishing. https://doi.org/10.1007/10_2014_288

Hollingshead, S., Kopec, J., Jackson, P. J., Davison, P. A., Dickman, M. J., Sobotka, R., … Hunter, C. N. (2012). Conserved chloroplast open-reading frame *ycf54* is required for activity of the magnesium protoporphyrin monomethylester oxidative cyclase in *Synechocystis* PCC 6803. *Journal of Biological Chemistry*, *287*, 27823–27833.

Kirst, H., Formighieri, C., & Melis, A. (2014). Maximizing photosynthetic efficiency and culture productivity in cyanobacteria upon minimizing the phycobilisome light-harvesting antenna size. *BBA - Bioenerg*, *1837*, 1653–1664. https://doi.org/10.1016/j.bbabio.2014.07.009

Kiyota, H., Okuda, Y., Ito, M., Yokota Hirai, M., & Ikeuchi, M. (2014). Engineering of cyanobacteria for the photosynthetic production of limonene from CO_2. *Journal of Biotechnology*, *185*, 1–7. https://doi.org/10.1016/j.jbiotec.2014.05.025

Ko, S. C., Lee, H. J., Choi, S. Y., Choi, J., & Woo, H. M. (2019). Bio-solar cell factories for photosynthetic isoprenoids production. *Planta*, *249*, 181–193. https://doi.org/10.1007/s00425-018-2969-8

Leonard, E., Ajikumar, P. K., Thayer, K., Xiao, W. -H., Mo, J. D., Tidor, B., … Prather, K. L. J. (2010). Combining metabolic and protein engineering of a terpenoid biosynthetic pathway for overproduction and selectivity control. *Proceedings of the National Academy of Sciences of the United States of America*, *107*, 13654–13659.

Lichtenthaler, H. K. (2007). Biosynthesis, accumulation and emission of carotenoids, alpha-tocopherol, plastoquinone, and isoprene in leaves under high photosynthetic irradiance. *Photosynthesis Research*, *92*, 163–179.

RIGHTSLINK

10970290, 2019, 8, Downloaded from https://analyticalsciencejournals.onlinelibrary.wiley.com/doi/10.1002/bit.26988 by University Degli Studi Di Vero, Wiley Online Library on [25/10/2024]. See the Terms and Conditions (https://onlinelibrary.wiley.com/terms-and-conditions) on Wiley Online Library for rules of use; OA articles are governed by the applicable Creative Commons License

Lichtenthaler, H. K. (2010). Biosynthesis and Emission of Isoprene, Methylbutanol and Other Volatile Plant Isoprenoids. In A. Herrmann (Ed.), *Chem. Biol. volatiles* (pp. 11–47). New York: John Wiley & Sons, Ltd.

Lin, P.-C., & Pakrasi, H. B. (2019). Engineering cyanobacteria for production of terpenoids. *Planta*, *249*, 145–154. http://link.springer.com/10.1007/s00425-018-3047-y

Lin, P.-C., Saha, R., Zhang, F., & Pakrasi, H. B. (2017). Metabolic engineering of the pentose phosphate pathway for enhanced limonene production in the cyanobacterium *Synechocystis* sp. PCC 6803. *Scientific Reports*, *7*, 1–10. https://doi.org/10.1038/s41598-017-17831-y

Lindberg, P., Park, S., & Melis, A. (2010). Engineering a platform for photosynthetic isoprene production in cyanobacteria, using *Synechocystis* as the model organism. *Metabolic Engineering*, *12*, 70–79. https://doi.org/10.1016/j.ymben.2009.10.001

McGarvey, D. J., & Croteau, R. (1995). Terpenoid metabolism. *The Plant Cell*, *7*, 1015–1026.

Melis, A. (2013). Carbon partitioning in photosynthesis. *Current Opinion in Chemical Biology*, *17*, 453–456. https://doi.org/10.1016/j.cbpa.2013.03.010

Melis, A. (2017). Terpene hydrocarbons production in cyanobacteria. In D. A. Los (Ed.), *Cyanobacteria – Omi. Manip* (pp. 187–198). U.K.: Caister Academic Press.

Miao, R., Xie, H., & Lindblad, P. (2018). Enhancement of photosynthetic isobutanol production in engineered cells of *Synechocystis* PCC 6803. *Biotechnology for Biofuels*, *11*, 267. https://doi.org/10.1186/s13068-018-1268-8

Nozzi, N. E., Case, A. E., Carroll, A. L., & Atsumi, S. (2017). systematic approaches to efficiently produce 2,3-butanediol in a marine cyanobacterium. *ACS Synthetic Biology*, *6*, 2136–2144. https://doi.org/10.1021/acssynbio.7b00157

Sage, R. F. (2002). Variation in the kcat of Rubisco in C3 and C4 plants and some implications for photosynthetic performance at high and low temperature. *Journal of Experimental Botany*, *53*, 609–620. https://doi.org/10.1093/jexbot/53.369.609.

Schwender, J., Gemünden, C., & Lichtenthaler, H. K. (2001). Chlorophyta exclusively use the 1-deoxyxylulose 5-phosphate/2-C-methylerythritol 4-phosphate pathway for the biosynthesis of isoprenoids. *Planta*, *212*, 416–423.

Wang, G., Tang, W., & Bidigare, R. R. (2005). *Terpenoids as therapeutic drugs and pharmaceutical agents. In:. Nat. Prod* (197–227). Springer.

Wang, X., Liu, W., Xin, C., Zheng, Y., Cheng, Y., Sun, S., … Yuan, J. S. (2016). Enhanced limonene production in cyanobacteria reveals photosynthesis limitations. *Proceedings of the National Academy of Sciences of the United States of America*, *113*, 14225–14230. http://www.ncbi.nlm.nih.gov/pubmed/27911807

Williams, J. G. K. (1988). Construction of specific mutations in Photosystem II photosynthetic reaction center by genetic engineering methods in *Synechocystis* 6803. *Methods in Enzymology*, *167*, 766–778.

Wise, M. L., & Croteau, R. (1999). Monoterpene biosynthesis. In D. E. Cane (Ed.), *Compr. Nat. Prod. Chem. Incl. carotenoids steroids* (pp. 97–153). Oxford: Elsevier science.

Zurbriggen, A., Kirst, H., & Melis, A. (2012). Isoprene production via the mevalonic acid pathway in *Escherichia coli* (bacteria). *Bioenergy Res*, *5*, 814–828.

SUPPORTING INFORMATION

Additional supporting information may be found online in the Supporting Information section at the end of the article.

How to cite this article: Betterle N, Melis A. Photosynthetic generation of heterologous terpenoids in cyanobacteria. *Biotechnology and Bioengineering*. 2019;116:2041–2051. https://doi.org/10.1002/bit.26988

10970290, 2019, 8, Downloaded from https://analyticalsciencejournals.onlinelibrary.wiley.com/doi/10.1002/bit.26988 by University Degli Studi Di Vero, Wiley Online Library on [25/10/2024]. See the Terms and Conditions (https://onlinelibrary.wiley.com/terms-and-conditions) on Wiley Online Library for rules of use; OA articles are governed by the applicable Creative Commons License

RIGHTSLINK